Journal of Materials and Environmental Science
ISSN : 2028-2508
e-ISSN : 2737-890X
CODEN : JMESCN

J. Mater. Environ. Sci., 2025, Volume 16, Issue 6, Page 968-981

http://www.jmaterenvironsci.com

Characterization and pozzolanic potential of sugarcane bagasse, coconut fiber and husk and oil palm ash from Côte d'Ivoire for sustainable substitution in cement

Irie Christian ZAMBLE[1*], Séka Simplice KOUASSI[1], Tohoué Monique TOGNONVI[2], Diby Benjamin OSSONON[2]**

1Laboratory of Environmental Science and Technology, University of Jean Lorougnon Guede, Daloa, Côte d'Ivoire
2Unit for Training and Research of Biological Sciences, University of Peleforo Gon Coulibaly, Korhogo, Côte d'Ivoire

**Corresponding author, Email address: zamble.christian01@ujlg.edu.ci*
***Corresponding author, Email address: sekasimplice@ujlg.edu.ci*

Received *17 Mar 2025,*
Revised *08 May 2025,*
Accepted *09 May 2025*

Keywords:
- ✓ *cementitious substitution;*
- ✓ *pozzolanic reactivity;*
- ✓ *ash characterization;*
- ✓ *construction materials;*
- ✓ *Circular economy*

Citation*: Zamble I. C., Kouassi Se. S., Tognovi T. M., Ossonon D. B. (2025) Characterization and pozzolanic potential of sugarcane bagasse, coconut fiber and husk and oil palm ash from Côte d'Ivoire for sustainable substitution in cement, J. Mater. Environ. Sci., 16(6), 968-981*

Abstract: This study explores the characteristics and pozzolanic potential of ashes from three types of agricultural waste in Côte d'Ivoire with a view to using their mixture as a substitute in cement. These are sugarcane bagasse (CBCS), coconut husks (CC) and oil palm husks (CPH). After calcining at 700°C for two hours, the ashes were subjected to analysis of their physical, chemical and microstructural properties to determine their suitability as partial cement substitutes. The results show that CBCS has an average particle size of 0.808 µm and a specific surface area of 80.93 m²/g, with a silica content of 75.65%, making it compliant with the requirements of ASTM C 618 for pozzolanic materials. CPH also has favorable characteristics, with an average size of 2.527 µm, a specific surface area of 251.83 m²/g and a silica content of 71.74%. Coconut ash, on the other hand, although having an average size of 6.308 µm and a specific surface area of 69.7 m²/g with a silica content of 67.9%, is less favorable. Microstructural analyses and pozzolanic activity tests confirm that CBCS and CPH are promising candidates for partial cement substitution, while CC has less favorable characteristics. The combined use of these ashes could substitute cement and contribute to more sustainable construction practices by reducing production costs and CO_2 emissions.

1. Introduction

Côte d'Ivoire's rapid economic development means a growing demand for modern infrastructure, leading to increased consumption of construction materials such as cement. However, cement production, whose main material is clinker, is very energy-intensive and emits large quantities of carbon dioxide (approximately one tone of CO_2 per ton of cement produced) (Davidovits (1991). The high cost of cement, exacerbated by the fact that clinker is produced at 1450 °C (Pacheco-Torgal *et al.* (2008), also limits its accessibility to a large proportion of the population.

With these environmental and economic challenges, research into alternative materials, such as artificial pozzolans (clay, calcined biomass, etc.), has expanded (Jabri *et al.* 2013; Tabaght *et al.* 2020; N'diaye *et al.* 2022; Olaiya *et al.* 2025). Pozzolans are materials rich in silica and alumina which, in the presence of lime, react to form cementitious compounds, thereby reducing the amount of clinker required and the associated CO_2 emissions (Donatello *et al.* (2010). Their use in partial substitution of cement has shown similar capabilities to traditional cements and in some cases improvements in strength, durability of mortars by increasing the amount of Hydrated Calcium Silicate (HSC) (Khedr and Abou-Zeid (1994), (Rukzon and Chindaprasirt (2012), (Tagnit-Hamou and Tognonvi (2015), (Mohammed (2017), and reduced environmental impact by reducing carbon dioxide (Ciach *et al.* (1971), (Ganesan *et al.* (2007), (Thomas *et al.* (2021).

The increasing use of agricultural waste in various industrial sectors, including the cement industry, has become common practice to promote the circular economy and reduce CO_2 emissions. Agricultural wastes, such as sugarcane bagasse, coconut fibers and husks, as well as oil palm fibers and husks, are valuable resources for partial replacement of cement due to their compositions (Gupta *et al.* (2022), Hamada *et al.* (2023), (Ranatunga *et al.* (2023). Their use not only makes it possible to reduce dependence on traditional natural resources, but also to reduce the carbon footprint of the cement industries, which is a major issue in the fight against climate change (Bheel *et al.* (2021). In addition, this practice makes it possible to use local resources and reduce dependence on non-renewable resources, thus promoting a more sustainable and ecological approach to cement production.

Studies carried out on this ash have shown excellent results in terms of its ability to replace cement (Neto *et al.* (2021), (De Sande *et al.* (2021), De Azevedo *et al.* (2022). Unfortunately, the individual use of this ash limits its use on a large scale.

In this context, a comparative study of the characteristics of the ashes of these agricultural wastes produced in Côte d'Ivoire is carried out to see the different strengths and weaknesses of these three ashes for the use of their mixture in the replacement of cement. The selection of these three specific wastes in the Ivorian context is motivated by their abundant availability, accessibility and potential to contribute to the transition towards more sustainable and environmentally friendly practices in the cement sector (GIZ (2020).

2. Material and methods

The raw materials used in this study are waste produced by industry and used as fuel for boilers. The final by-product, ash, is dumped on roads and fields. The ash is not recycled in any particular way, despite its large quantity, which may be justified for industrial use.

2.1 Material

The different ashes produced are shown in **Figure 1**.

A company located about 115 km from the town of Daloa (Côte d'Ivoire) supplied sugar cane bagasse. It represents about 25% of the sugar cane produced (Ouedraogo *et al.* (2022). The bagasse used for calcination comes from boilers where it has not been completely calcined and sieved to eliminate contaminants due to the collection and preservation process.

The coconut fibers were collected from coconut traders in the same town. Those used for ash production were washed and dried in an oven for 24 hours at 105°C to eliminate contaminants and water.

The oil palm husks and fibers were collected from the town's restaurant owners. The oil palm husks and fibers used for calcination were washed and air-dried for several days to eliminate contaminants and water. Then they underwent incomplete combustion in the open air for 01 day to facilitate the grinding and calcination of the husk.

The three agricultural wastes were calcined in a Nabertherm P330 oven at a temperature of 700°C, with a heating rate of 10°C/min for 02 hours. After calcination, the oven and its contents were subjected to normal oven cooling in the laboratory. All the ash obtained was sieved to 200 µm.

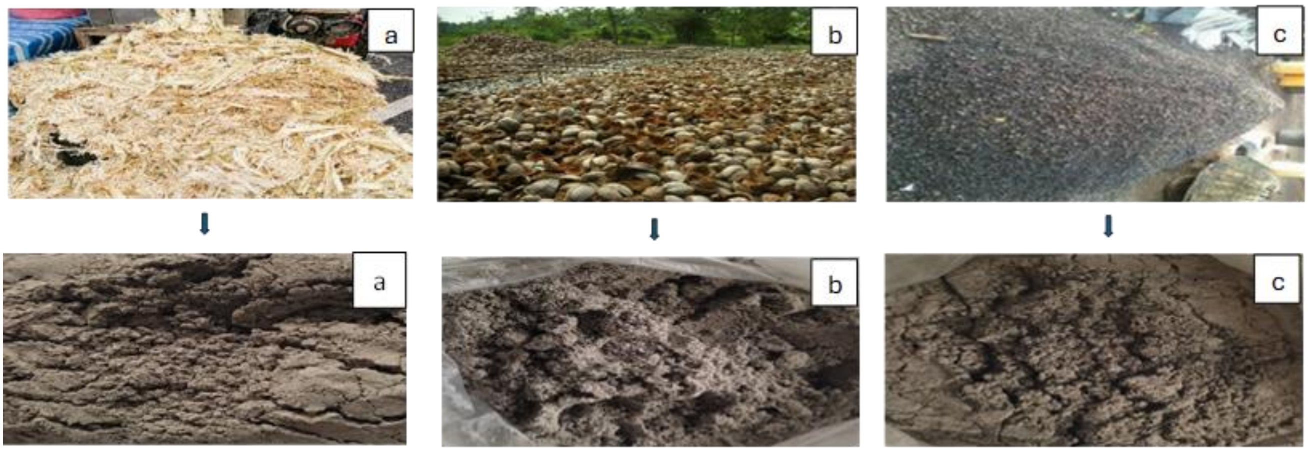

Figure 1. a) sugar cane bagass ash, b) coconut fiber and shell ash, c) oil palm shell ash

2.2 Methods

2.2.1 Chemical, mineralogical and physical properties

Average particle size and zeta potential were determined by laser particle sizing using DLS and the Zetasizer Advance. The zeta potential measures the ability of a particle suspended in a liquid to stay stable. It also represents the electrical charge in the suspension. The dynamic light scattering technique was used to obtain the zeta potential and mean size from the peak of the particle size distribution of the sample. This technique can be used to measure the particle size of molecules in a range from 0.3 nm to 10 mm (Jeffry *et al.*, 2018). Pore size and volume were determined because of specific surface area determination using the H-K (Original and Saito-Foley) and NLDFT (Non-Local Density Functional Theory) methods. The specific surface area was evaluated by the BET method using an automated volumetric nitrogen adsorption apparatus of the TMAXCN type (TMAX-BSD-PM2).

The chemical composition was obtained using inductively coupled plasma mass spectroscopy (ICP-MS). The crystalline and amorphous phases, crystallographic orientation and texture of the ashes were determined using X-ray diffraction. X-ray diffraction was recorded with a Bruker diffractometer using a Cu Kα radiation source. The different vibrations and functional groups of the ash were determined using a Fourier transform infrared spectrometer. The infrared spectrometer used to identify the functional groups of the minerals was a Thermo Scientific Nicolet 6700. High-resolution microscopic images of the ash surface were obtained using a Tescan LYRA 3 XMH scanning electron microscope.

2.2.2 Pozzolanic activity

Chemical, mineralogical and mechanical methods can be used to determine pozzolanic activity. The chemical method known as the Frattini Test was used. The tests are carried out in accordance with BS EN 196-5 and the results are plotted on the solubility curve.

3. Results and Discussion

3.1 Physical, chemical and physic-chemical properties

The physical properties of CBCS, CC and CPH are shown in **Table 1**. Data observed from **Table 1** indicate that CBCS, CC and CPH particles have mean sizes of 0.81, 6.31 and 2.53 µm respectively.

The small average size of 0.81 µm for CBCS means that it has a good fineness, which could make it easier to dissolve. The value obtained is lower than that of the CBCS studied in previous investigations (Thomas *et al.* (2021), which ranged from 76.3 to 1.7 µm, of 26.16 µm found in Burkina Faso (Ouédraogo *et al.* (2022) and of 36.68 µm observed despite 08 hours of calcination of the bagasse at 600°C (Neto *et al.* (2021) in Brazil. In addition, it's larger than what found in India with a D_{50} between 0.11 and 0.21 µm (Teja *et al.* (2017) lower but much closer to those found in our study.

The small average size of 6.31 µm of the CC also means that coconut ash has a good fineness which could make it easier to put into solution. The value obtained is within the range of sizes of coir ash studied which are 0.53 µm and 0.4 mm (Arimanwa *et al.* (2020), (Kassar and Momoh (2018) or the study conducted in Nigeria (Kassar and Momoh (2018) was carried out on palm hulls while that involved a mixture of fiber and hull with a large majority of fiber calcined at 600°C for about 10 hours (Arimanwa *et al.* (2020). It is smaller than the 16.9 µm (Ranatunga *et al.* (2023) and larger than the 57.7 nm (Jeffry *et al.* (2018) after 15 hours of grinding. In addition, the size of the CC is much smaller than the 16.3 µm and 12.54 µm of fly ash generally used in cement replacement (Sua-iam and Chatveera (2021), (Padavala *et al.* (2024).

The average size of 2.51 µm observed in HPC means that the ash has good fineness. The values of 0.98 µm obtained after grinding and calcination at 1000°C in Malaysia are larger (Hamada *et al.* (2020). This difference in size is due to the higher calcination temperature in the second case. In fact, the particle size distribution is influenced by the temperature above 750°C (Ouédraogo *et al.* (2022). A much smaller average size between 20 and 90 nm was observed after 30 hours of grinding (Rajak *et al.* (2015). In a review (Hamada *et al.* (2021), average sizes of between 1.07 and 22.78 µm, the range in which the size of CPH is found.

We can therefore see that CBCS has the smallest size, followed by CPH and finally CC. The larger size of CC is due to storage conditions. In fact, the CC has the finest particles when it leaves the kiln. During the storage of the different ashes, the very fine particles of CC tend to form a mass and agglomerate by capturing the ambient humidity, resulting in larger particles. The smaller size of CBCS compared with CPH is due to the difference in the raw material used. The bagasse used to produce the ash is a less dense and solid fibrous residue than the hulls used to produce CPH. The average size of all the ashes is less than the value of 10 µm adopted by most researchers as the maximum characteristic size to obtain adequate pozzolanic activity (Ouédraogo *et al.* (2022).

The surface characteristics of each sample, such as size distribution (porosity) and micropore volume, were determined and presented in **Table 1**. Micropore size decreases from CC through CPH to CBCS with values ranging from 1.41 to 0.74 nm while micropore volume decreases from CPH through CBCS to CC with values ranging from 0.0024 to 0.1435 ml/g. Although CC has the largest micropore size, it also has the smallest micropore volume. This is due to the agglomeration of hygroscopic particles that fill the void, reducing the remaining micropore volume. It can also be seen that the CPH micropore sizes are very close, while their micropore volumes are very far apart. This large difference in micropore volume could be explained by the fact that bagasse ash, due to its storage environment, captures moisture which reduces the volume of its micropores.

From these surface characteristics we can clearly conclude that CC has a much higher hygroscopic power, followed by CBCS and finally CPH.

Table 1 also gives the BET specific surface areas of the ashes. The specific surface area of 80.93 m^2/g for CBCS confirms its high reaction capacity. The value obtained is almost triple the 35.2 and 25.4 m^2/g for higher average sizes (Cordeiro *et al.* (2018). The specific surface area of 6.97 m^2/g of the CC means that the ash is able of active reaction although less so due to its hygroscopicity. The value obtained is very low compared to the 112.74 m^2/g (Jeffry *et al.* (2018). However, it's much higher than the 0.3566 m^2/g (Sua-iam and Chatveera (2021) and 0.863 m^2/g (Priya and Padmanaban (2023). The specific surface area of 251.83 m^2/g of CPH shows that the ash has a high reactive capacity. A specific surface area of 145.35 m^2/g after 30 hours of grinding despite the smaller size (Rajak *et al.* (2015). In a review (Hamada *et al.* (2021), the mean sizes between 1.07 and 22.78 µm for specific surface areas of between 0.4562 and 7205 m^2/g were reported. The results obtained in this study are well within the range.

These values testify to the fineness and high reactive capacity of the ash. They are consistent with the size, volume and particle size. Indeed, the specific surface area is a characteristic that is highly dependent on these three parameters. It is therefore much greater for particles with much smaller average sizes, high porosity and high pore volume. The lower specific surface area of CC is justified by its much larger size and much smaller micropore volume, even though it has the highest porosity due to the mass of its particles reacting with each other. The higher specific surface area of CPH than CBCS is due to the much larger micropore size and volume of CPH than CBCS, although the average particle size of CBCS is smaller. The zeta potential and conductivity of each ash are given in **Table 2**.

Table 1. Summary table of particle size data for CBCS, CC and CPH

Samples	CBCS	CC	CPH
Z-Average moyen (µm)	0,81	6,31	2,53
Micropore volume (ml/g)	0,0295-0,0409	0,0024	0,0944-0,1435
Micropore size (nm)	0,74 - 1,22	1,41	0,75 – 1,33
Specific BET surface area (m^2/g)	80,93	6,97	251,83

Table 2. Summary table of ionic data

Samples	CBCS	CC	CPH
Average zeta potential (mV)	-33,24	-16,9	-14,97
Conductivity (mS/cm)	1,75	4,40	0,38

The negative mean zeta potential of the three ashes indicates the presence of anions in the solutions or the desorption of positive ions. This characteristic indicates that all the ashes have a stable suspension, which could increase their stability during mixing. For particles of material to be stable in a mixture, it is essential that they have the same electrical charge. CBCS has -33.24 mV, more than double the zeta potentials of CC and CPH -16.9 and -14.97 mV respectively. The higher value for CBCS could be explained by the greater suspension of particles. Conductivity reflects a particle's ability to carry electrical charges. It is highest for CC with 4.40 mS/cm, followed by CBCS with 1.75 mS/cm and CPH with 0.38 mS/cm. The greater capacity of the particles to transport electrical charges in the CC solution may be due to the higher presence of ions in this solution than in the CBCS and CPH solutions.

3.2 Chemical and mineralogical composition of ashes

Table 3 gives the elemental chemical composition of the ash from CBCS, CC, and CPH. It shows that the ash generally comprises SiO_2, CaO, and K_2O in larger quantities. The high and predominant SiO_2 proportions of 75.65% for CBCS, 71.74% for CPH, and 67.9% for CC are certainly due to the consumption of ortho-silicic acid contained in West African soils by plants during their growth (Ouédraogo *et al.* (2022). The difference in samples is responsible for the difference in values.

The sum of SiO_2 + Al_2O_3 + Fe_2O_3 greater than 70% obtained for CBCS agrees with several studies conducted (Janjaturaphan and Wansom (2010), (Cordeiro *et al.* (2018), (Thomas *et al.* (2021), (Ouedraogo *et al.* (2022).

The sum of SiO_2 + Al_2O_3 + Fe_2O_3 obtained for CC agrees with studies conducted by (Abdalla *et al.* (2022), (Bheel *et al.* (2021), (Priya & Padmanaban (2023), (Islam *et al.* (2016). SiO_2 values for CC range from 5.23% to 88.62% (Anifowoshe and Nwaiwu (2016), (Arimanwa *et al.* (2020), (Bheel *et al.* (2021), (Gummadi and Srikanth (2016), (Isah (2014), (Madakson *et al.* (2012), (Sen and Chandak, 2015), (Taku (2012), (Umamaheswari and Vigneshkumar (2018), (Vasanthi *et al.* (2020). The lowest value was obtained after calcination at 600°C for 06h by (Arimanwa et *al.* (2020) and the highest value between 600 and 700°C for an unspecified time (Anifowoshe and Nwaiwu (2016).

The sum of SiO_2 + Al_2O_3 + Fe_2O_3 obtained for CPH is greater than the minimum requirement of 70% to be a type N pozzolan (ASTM C618 (2008) which agrees with several studies (Hamada *et al.* (2023), (Hamada (2020), (Islam *et al.* (2016). The sum of SiO_2 + Al_2O_3 + Fe_2O_3 in the ash of 77.58% and 72.75% respectively for CBCS and CPH is greater than the minimum requirement of 70% to be a Type N pozzolan (ASTM C618 (2008). As for CC, the sum of 69.1% is very close to the required 70%. This characteristic indicates that CBCS may have better reactivity and resistance than CPH and CC. In fact, the high percentage of SiO_2 contained in the ash could improve cement hydration and form the additional adhesive required in mortar production, thereby increasing strength. The high CaO content indicates that the hydraulic reactivity of the ash could be significant. Furthermore, the high K_2O and Na_2O content of the ash, certainly due to the use of fertilisers during cultivation, could considerably affect the strength and durability of the mortars through alkali-silica reactions (Ouédraogo *et al.* (2022). Also, the losses on ignition of 21.59% for CPH and 36.05% for CC could reduce the reactivity and resistance of the ashes with respect to CBCS, which is more acceptable at 11.38%.

Table 3. Summary table of the chemical composition of CBCS, CC and CPH

Oxide	SiO_2	Al_2O_3	Fe_20_3	CaO	K_2O	MgO	Na_2O	B_2O_3	BaO	MnO	L.O.I
CBCS	75.65	1.14	0.79	12.63	5.85	0.92	2.13	0.7	0.19	-	11.38
CC	67.9	0.84	0.36	18.74	-	0.9	7.77	1.93	1.56	-	36.05
CPH	7174	0.51	0.5	15.31	3.22	1.62	4.95	1.2	0.84	0.11	21.59

Figure 2 shows the CBCS, CC and CPH diffractograms. The crystalline phases identified in the three ashes are silica (SiO_2) and calcite ($CaCO_3$). The diffractograms of the three ashes confirm the presence of most of the silica, as indicated by the chemical analysis. The presence of silica in the form of quartz in the three ashes is probably due to contamination of the waste during collection, processing and storage.

The silica present in the CBCS sample is confirmed by the study of (Abdalla *et al.* (2022). Quartz and calcite are confirmed by (Gupta *et al.* (2022). Other phases such as microline, mullite and crystobalite have also been observed (Cordeiro *et al.* (2018), (Janjaturaphan and Wansom (2010), (Payá *et al.* (2002). That present in the CC sample is confirmed by the study of (Madakson *et al.* (2012) despite the absence of Cordierite, ($Mg_2Al_4Si_5O_{18}$) and that of the CPH is confirmed by (Hamada (2020), (Nagaratnam *et al.* (2019), (Salih *et al.* (2015), (Zeyad *et al.* (2016 & 2017). The large deviation from the baseline indicates the presence of a significant amount of amorphous silica in CBCS and CPH. In CC, on the other hand, the small deviation from the line confirms the low presence of amorphous phase, which could significantly reduce the reactivity of CC. The broad halo is more characteristic of CPH, indicating its greater amorphous phase, thus confirming the higher specific surface area obtained in **Table 1**.

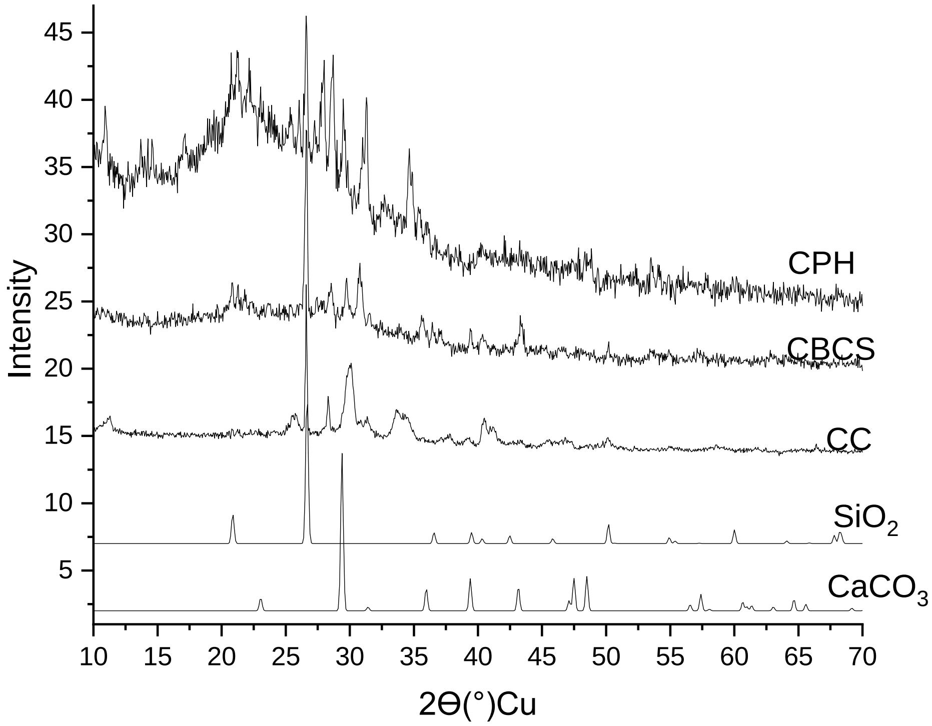

Figure 2. Diffractograms of CBCS, CC and CPH

3.3 Ashes functional groups

Figure 3 shows CBCS, CC and CPH infrared spectra. CBCS and CPH have identical peaks typical of siliceous materials (Farcas and Touzé (2001) for 1030 cm^{-1}, (Salih *et al.* (2015) with a slight difference around 3000 cm^{-1}. The Si-O vibrations observed at 1010 and 1030 cm^{-1} and the mean peak at 977 cm^{-1} for CBCS, CPH and CC respectively are due to the presence of silica (Khan *et al.* (2016). These observations thus confirm the results of the chemical analysis and the XRD. The broad stretching between 3400 and 2950 cm^{-1} shown in all spectra is attributed to the O-H stretching. It is more prominent in the CC sample, characteristic of water molecules trapped or adsorbed in the structure (Katte et al. (2023). This observation reflects the hygroscopic nature of the material, revealed by the large size and small volume of the micropores. The broad, non-existent peak of CPH in the same area reflects its low water-holding capacity compared with CBCS, which has a low hygroscopicity. This observation agrees with the order of hygroscopicity of ash shown in **Table 1.** Four peaks and a dome were detected in the analysis of the Fourier-transformed infrared spectrum of the CC as shown in **Figure 3**. The result showed that the presence of quartz and amorphous phase in the original ash gives a series of peaks located by a doublet at 1460 and 1370 cm^{-1} confirmed by (Madakson *et al.* (2012) where these overlap in the region between 1200 and 1434.12 cm^{-1}. **Table 4** shows the various peaks and their interpretations.

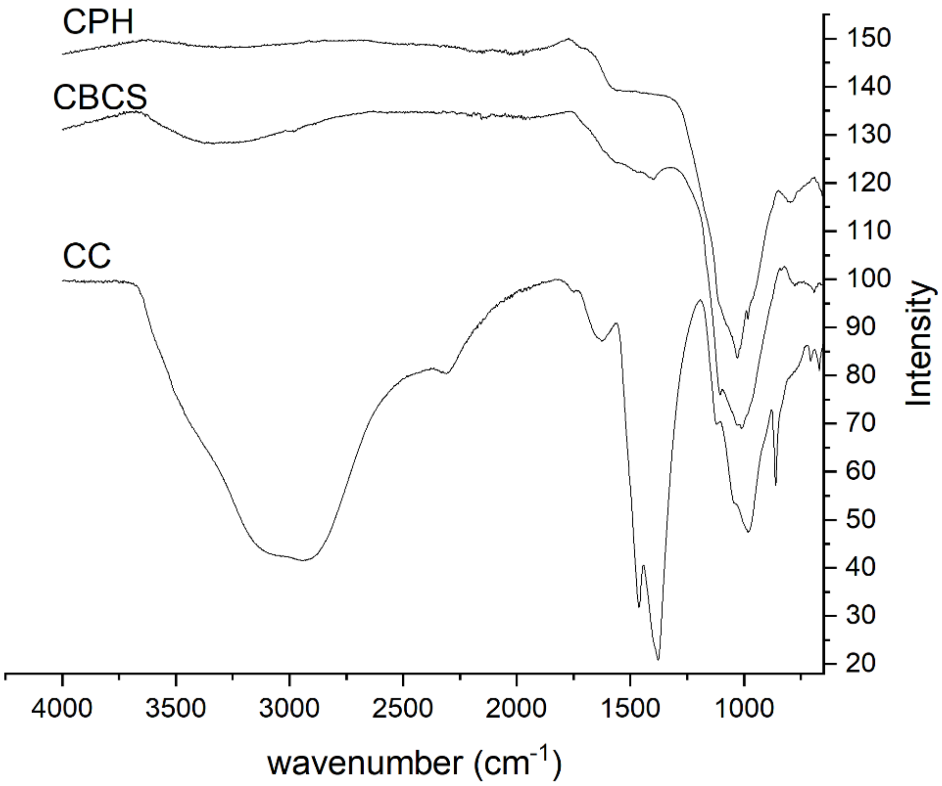

Figure 3. IR spectrum of CBCS, CC and CPH

Table 4. Summary spectrum analysis table

Samples	Intensity (cm^{-1})	Strip shape	Interatomic bonds	Elements present
CC	3080-2950	Doublet	ν O-H	Water
	1750	Weak	ν C-O (Silva et al. (2017)	Carbonyl
	1630	Weak	δ H-O-H (Frías et al. (2011)	Water
	1460-1370	Doublet	ν C-O (Silva et al. (2017)	Carbonyl
CBCS	3350	Large and medium	ν O-H (Frías et al. (2011)	Water
	1400	Medium	ν C-H (Ouedraogo et al. (2022)	Organic
	1010	Large and intense	ν Si-O (Ouedraogo et al. (2022) for 1000 ;	Silica
	690	Low	ν Si-O-Si and/or ν Si-O-Al (Ouedraogo et al. (2022)	Silica/alumina
CPH	3240	Large and low	ν O-H (Khan et al. (2016) for 434 cm^{-1} ; (Farcas and Touzé (2001) for 3540-3400 cm^{-1}	water
	1030	Large and intense	ν Si-O (Farcas and Touzé (2001) for 1030 cm^{-1} ; (Salih et al. (2015)	Silica

3.5 Ashes surface morphology

The morphology of CBCS, CC and CPH particles was observed from the SEM as shown in **Figure 4.** Examination of their microstructural properties is essential to understand how they modify the behavior of the mortar. **Figure 3** shows that CC and CPH ash particles have slightly more homogeneous shapes in contrast to CBCS which has uneven shapes and varied sizes at the 20µm scale. The more homogeneous images of coconut ash agree with (Madakson *et al.* (2012), (Priya and Padmanaban (2023) and (Ranatunga *et al.* (2023). This observation proves the high zeta potential obtained in CBCS, and the close values obtained in CC and CBCS. As CBCS particles are more irregular, dissolving them will create much larger suspensions, thus increasing the zeta potential. These large irregular cheese particles due to the presence of imbricated fiber have been observed in several studies (Abdalla *et al.* (2022), (Gupta and Kumar (2022), (Thomas *et al.* (2021). On a smaller scale, most ashes show a typical silica fume surface which is characteristic of the presence of silica in all samples (Abdalla *et al.* (2022). The presence of this surface could increase the pozzolanic potential of the ash. A compact ball is observed in the middle of the CC image.

This observation confirms the massing and agglomeration of these very fine particles.

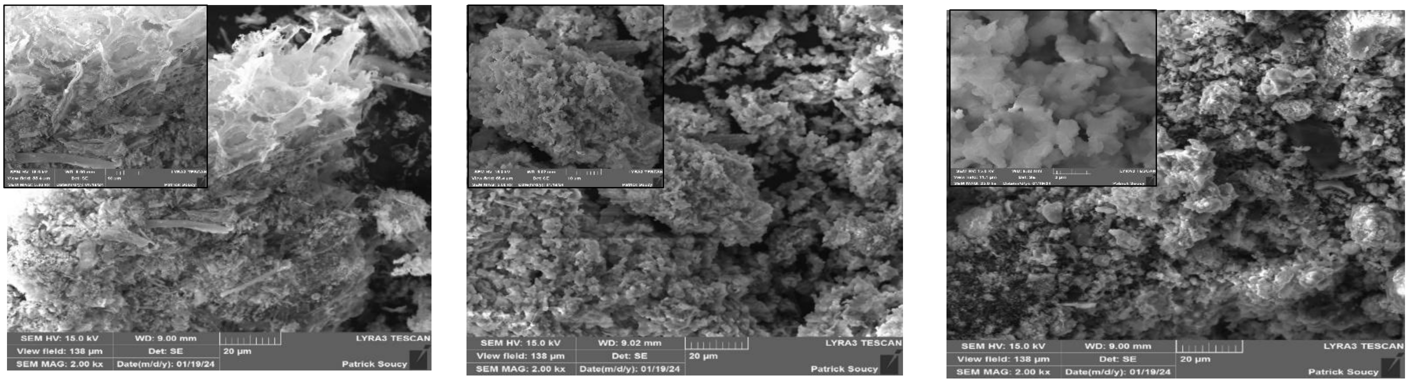

CBCS à 20µm CC à 20µm CPH à 20µm

Figure 4. Scanning electron microscope image

3.6 Pozzolanic activity assessments

Figure 5 shows the results of the Frattini ash tests based on the solubility curve. Pozzolanic activity is defined as the ability of a predominantly silica pozzolan to react with free lime to form calcium silicate hydrate (CSH). **Figure 5** shows that the coordinates of CPH and CBCS are below curve the solubility. This means that both samples have pozzolanic activity and can be considered as pozzolans in accordance with ASTM C 618, confirmed by chemical analysis. Due to the range of values for the concentration of hydroxide ions, the coordinates of the CC could not be represented on the figure. **Figure 5** also shows the different pairs of ash coordinates. The results obtained in the Frattini test indicate that the addition of CBCS, CC and CPH reduces the content. Pozzolanic activity is defined as the ability of a predominantly silica pozzolan to react with free lime to form calcium silicate hydrate (CSH). **Figure 5** shows that the coordinates of CPH and CBCS are below the solubility curve. This means that both samples have pozzolanic activity and can be considered as pozzolans in accordance with ASTM C 618, confirmed by chemical analysis. It's easy to see that CC has a hydroxide ion concentration of 226.63 mmol/l, followed by CBCS with 89.65 mmol/l and CPH with 49.31 mmol/l. This order of concentration values is confirmed by the order of conductivity obtained in **Table 2**. The higher value for CC is due to its high hygroscopic power, which allowed it to dissolve more water, favoring the dissolution of hydroxide and hydronium ions.

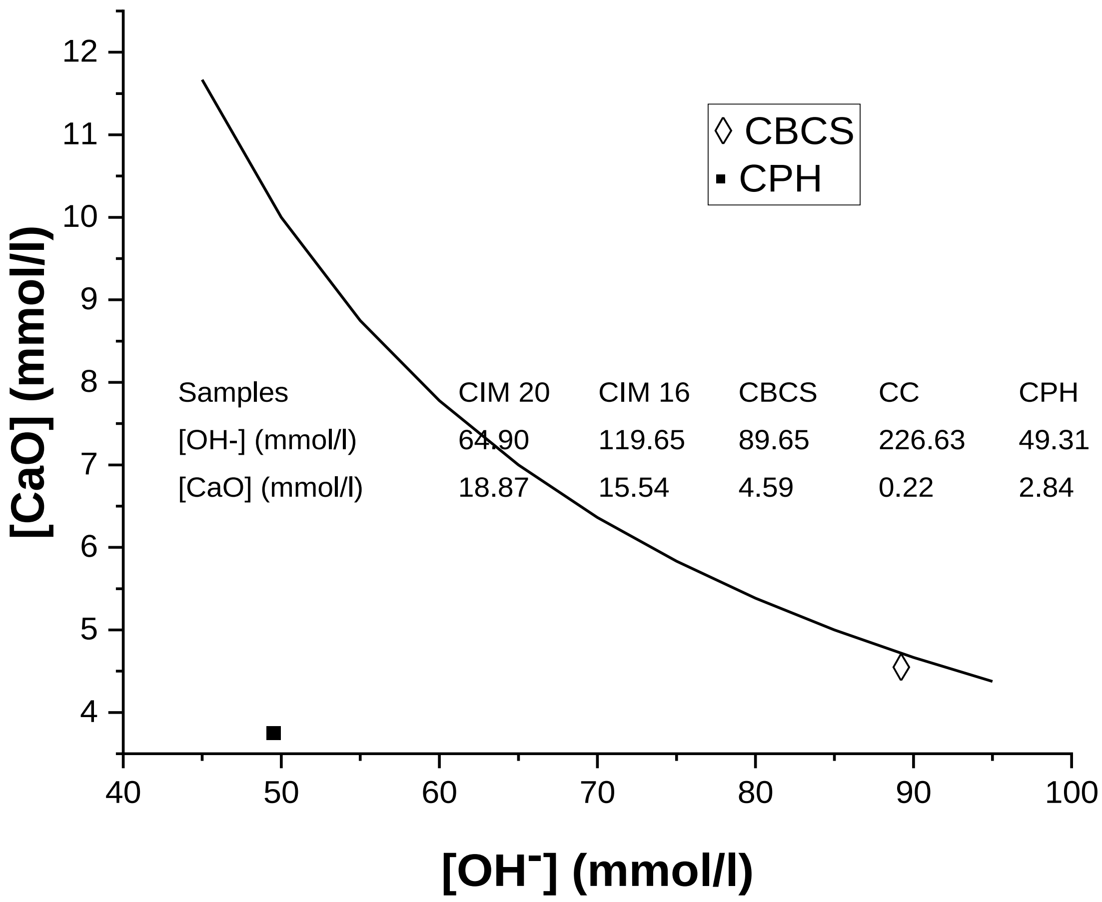

Figure 5. Frattini test result

Conclusion

This comparative study highlighted the potential of sugarcane bagasse (CBCS), coconut fiber and husk (CC) and oil palm husk (CPH) ash in Côte d'Ivoire as sustainable substitutes in cement production. Particle size analysis revealed that CBCS ash had the smallest average particle size (0.808 µm), followed by CPH ash (2.53 µm) and finally CC ash (6.31 µm). BET specific surface area are showed that CPH ash had the largest surface area (251.83 m^2/g), followed by CBCS (80.93 m^2/g) and CC (6.97 m^2/g), indicating better fineness and greater reactive capacity for CBCS and CPH.

The chemical composition of the ashes showed a predominance of silica (SiO_2) in all samples, with proportions of 75.65% for CBCS, 71.74% for CPH, and 67.9% for CC. CBCS and CPH ash also showed high CaO contents (12.63% and 15.31% respectively), which is beneficial for the pozzolanic reaction.

Scanning electron microscopy (SEM) analysis revealed that CC and CPH particles have more homogeneous shapes, while CBCS particles are more irregular. This heterogeneity in the shape of CBCS particles could influence their behavior in cement mixes, but their small size and high specific surface area could compensate for this disadvantage.

Frattini's tests confirmed that CBCS and CPH ashes have significant pozzolanic activity, making them suitable for use as partial cement substitutes. As for CC ash, it showed the greatest power to consume the lime contained in cement, thus confirming its acceptable pozzolanic potential despite the lesser characteristics observed. In addition, its availability and acceptable chemical composition make it a viable option.

In conclusion, sugarcane bagasse (CBCS), coconut fiber and husk (CC) and oil palm husk (CPH) ashes show good potential for use as partial cement substitutes, thanks to their favorable physical, chemical and microstructural properties. The combination of these ashes is well feasible and could offer a sustainable solution for reducing cement production costs and lowering the carbon footprint, thus contributing to greener construction practices in Côte d'Ivoire. This study provides a solid basis for encouraging the adoption of these alternative materials in the construction sector, paving the way for ecological and economic innovations.

Acknowledgement: The technical inputs of Mr. ZAMBLE Bi for financing.

Disclosure statement: *Conflict of Interest:* The authors declare that there are no conflicts of interest.
Compliance with Ethical Standards: This article does not contain any studies involving human or animal subjects.

References:

Abdalla T. A., Koteng D. O., Shitote S. M., Matallah M. (2022) Mechanical and durability properties of concrete incorporating silica fume and a high volume of sugarcane bagasse ash, *Results in Engineering*, 16, 100666. https://doi.org/10.1016/j.rineng.2022.100666

Anifowoshe F., Nwaiwu N. (2016) The use of coconut fiber ash as a partial replacement for cement, *British Journal of Applied Science & Technology*, 17(5), 1-11. https://doi.org/10.9734/BJAST/2016/25926

Arimanwa M. C., Anyadiegwu P. C., Ogbonna N. P. (2020) The potential use of Coconut Fiber Ash (CFA) in concrete, *The International Journal of Engineering and Science (IJES)*, 9(1), 68-75.

Bheel N., Mahro S. K., Adesina A. (2021) Influence of coconut shell ash on workability, mechanical properties, and embodied carbon of concrete, *Environmental Science and Pollution Research*, 28(5), 5682-5692. https://doi.org/10.1007/s11356-020-10882-1

Bheel N., Mangi S. A., Meghwar S. L. (2021) Coconut shell ash as cementitious material in concrete : a review, *Jurnal Kejuruteraan*, 33(1), 27-38. https://doi.org/10.17576/jkukm-2021-33(1)-03

Ciach T. D., Gillott J. E., Swenson E. G., Sereda P. J. (1971) Microstructure of calcium silicate hydrates, *Cement and Concrete Research*, 1(1), 13-25. https://doi.org/10.1016/0008-8846(71)90080-9

Cordeiro G. C., Barroso T. R., Toledo Filho R. D. (2018) Enhancement the properties of sugar cane bagasse ash with high carbon content by a controlled re-calcination process, *KSCE Journal of Civil Engineering*, 22(4), 1250-1257. https://doi.org/10.1007/s12205-017-0881-6

De Azevedo A. R. G., Amin M., Hadzima-Nyarko M., Agwa S. I., Zeyad A. M., Tayeh B. A., Adesina A. (2022) Possibilities for the application of agro-industrial wastes in cementitious materials: A brief review of the Brazilian perspective, *Cleaner Materials*, 3, 100040. https://doi.org/10.1016/j.clema.2021.100040

De Sande T. V., Sadique M., Pineda P., Bras A., Atherton W., Riley M. (2021). Potential use of sugar cane bagasse ash as sand replacement for durable concrete, *Journal of Building Engineering*, 39, 102277. https://doi.org/10.1016/j.jobe.2021.102277

Donatello S., Tyrer M., Cheeseman C. R. (2010) Comparison of test methods to assess pozzolanic activity, *Cement and Concrete Composites*,32(2),121-127. https://doi.org/10.1016/j.cemconcomp.2009.10.008

Farcas F., Touzé P. (2001) La spectrométrie infrarouge à transformée de Fourier (IRTF). *Bulletin des laboratoires des ponts et chaussées*, 230(4350), 77-88.

Frías M., Villar E., Savastano H. (2011) Brazilian sugar cane bagasse ashes from the cogeneration industry as active pozzolans for cement manufacture, *Cement and Concrete Composites*, 33(4), 490-496. https://doi.org/10.1016/j.cemconcomp.2011.02.003

Ganesan K., Rajagopal K., Thangavel K.(2007). Evaluation of bagasse ash as supplementary cementitious material. *Cement and Concrete Composites*, 29(6), 515-524. https://doi.org/10.1016/j.cemconcomp.2007.03.001

Gummadi C., Srikanth G. (2016) Experimental Investigation on Partial Replacement of Cement with Coconut shell ash and silica fume in concrete, *Journal of Advances in Science and Technology*, 11(23), 7-15.

Gupta C. K., Sachan A. K., Kumar R. (2022) Utilization of sugarcane bagasse ash in mortar and concrete: A review, *Materials Today: Proceedings*, 65(2), 798-807. https://doi.org/10.1016/j.matpr.2022.03.304

Hamada H. M., Abed F., Alattar A., Yahaya F. M., Tayeh B. C., Aisheh Y. I. A. (2023). Influence of palm oil fuel ash on the high strength and ultra-high-performance concrete: A comprehensive review, *Engineering Science and Technology, an International Journal*, 45, 101492. https://doi.org/10.1016/j.jestch.2023.101492

Hamada H. M., Al-attarb A. Al., Yahaya F. M., Muthusamy K., Tayeh B. A., Humada A. M. (2020) Effect of high-volume ultrafine palm oil fuel ash on the engineering and transport properties of concrete, *Case Studies in Construction Materials*,12, e00318. https://doi.org/10.1016/j.cscm.2019.e00318

Hamada H. M., Jokhio G. A., Yahaya F. M., Humada A. M., Gul Y. (2018) The present state of the use of palm oil fuel ash (POFA) in concrete, *Construction and Building Materials*, 175, 26-40. https://doi.org/10.1016/j.conbuildmat.2018.03.227

Hamada H. M., Thomas B. S., Yahaya F. M., Muthusamy K., Yang J., Abdalla J. A., Hawileh R. A. (2021). Sustainable use of palm oil fuel ash as a supplementary cementitious material: A comprehensive review, *Journal of Building Engineering*, 40, 102286. https://doi.org/10.1016/j.jobe.2021.102286

Isah B. W.(2014) Effect of Coconut Shell Ash on Properties of Fired Clay Brick, *Journal of Civil Engineering and Environmental Technology*, 1(6), 7-11.

Islam U. Mo. M., Mo K. H., Alengaram U. J., Jumaat M. Z. (2016) Durability properties of sustainable concrete containing high volume palm oil waste materials, *Journal of Cleaner Production*, 137, 167-177. https://doi.org/10.1016/j.jclepro.2016.07.061

Jabri M., Mejdoubi E., El Gadi M., Hammouti B. (2013), Hydratation mechanism of a zinc phosphate cement and development of its mechanical profile, *Res. Chem. Intermed.*, 39 N°7, 3117-3126.

Janjaturaphan S., Wansom S. (2010) Pozzolanic activity of industrial sugar cane bagasse ash, *Suranaree J. Sci. Technol.*, 17(4), 349-357.

Jeffry S. N. A., Jaya R. P., Hassan N. A., Yaacob H., Mirza J., Drahman S. H. (2018) Effects of nanocharcoal coconut-shell ash on the physical and rheological properties of bitumen, *Construction and Building Materials*, 158, 1-10. https://doi.org/10.1016/j.conbuildmat.2017.10.019

Kassar T., Momoh E. (2018) Effect of coconut shell ash on the sulphate resisting capabilities of concrete, *International Journal and Advanced Engineering Research and Technology (IJAERT)*, 6(6), 393-399.

Katte A. R., Mwero J., Gibigaye M., Koteng D. O. (2023) Recycling palm oil wastes for the production of a pozzolanic cement replacement material for concrete, *Results in Engineering*, 17, 100903. https://doi.org/10.1016/j.rineng.2023.100903

Khan I. U., Bhat A. H., Masset P. J., Khan F. U., Rehman W. U. (2016) Synthesis and characterization of palm oil fuel ash (POFA) and metakaolin based geopolymer for possible application in nanocoating, *AIP Conf. Proc.*, 1787(1), 050009. https://doi.org/10.1063/1.4968107

Khedr S. A., Abou-Zeid M. N. (1994) Characteristics of silica-fume concrete, *Journal of Materials in Civil Engineering*, 6(3), 357-375. https://doi.org/10.1061/(ASCE)0899-1561(1994)6:3(357)

Madakson P. B., Yawas D. S., Apasi A. (2012) Characterization of coconut shell ash for potential utilization in metal matrix composites for automotive applications, *International Journal of Engineering Science and Technology (IJEST)*, 4(3), 1190-1198.

Mohammed S. (2017) Processing, effect and reactivity assessment of artificial pozzolans obtained from clays and clay wastes: A review, *Construction and Building Materials*, 140, 10-19. https://doi.org/10.1016/j.conbuildmat.2017.02.078

Nagaratnam B. H., Mannan M. A., Rahman M. E., Mirasa A. K., Richardson A., Nabinejad O. (2019) Strength and microstructural characteristics of palm oil fuel ash and fly ash as binary and ternary blends in Self-Compacting concrete, *Construction and Building Materials*, 202, 103-120. https://doi.org/10.1016/j.conbuildmat.2018.12.139

N'diaye A.D., Kankou M.S.A., Hammouti B., Nandiyanto A.B.D., Al Husaeni D.F. (2022). A review of biomaterial as an adsorbent: From the bibliometric literature review, the definition of dyes and adsorbent, the adsorption phenomena and isotherm models, factors affecting the adsorption process, to the use of typha species waste as adsorbent. *Communications in Science and Technology*, 7(2), 140-153. https://doi.org/10.21924/cst.7.2.2022.977

Neto A. J. D. S., De França M. J. S., Amorim J. N. S. D., Ribeiro D. V. (2021) Effects of adding sugarcane bagasse ash on the properties and durability of concrete, *Construction and Building Materials*, 266, 120959. https://doi.org/10.1016/j.conbuildmat.2020.120959

Norme ASTM Standard (2008), C618 standard specification for coal fly Ash and raw or calcined natural pozzolan for use in concrete, *Annual Book of ASTM standards, ASTM International* (West Conshohocken).

Olaiya, B.C., Lawan, M.M., Olonade, K.A. et al. An overview of the use and process for enhancing the pozzolanic performance of industrial and agricultural wastes in concrete. *Discov Appl Sci* 7, 164 (2025). https://doi.org/10.1007/s42452-025-06586-1

Ouedraogo M., Sawadogo M., Sanou I., Barro M., Nassio S., Seynou M., Zerbo L. (2022). Characterization of sugar cane bagasse ash from Burkina Faso for cleaner cement production: Influence of calcination temperature and duration, *Results in Materials*, 14, 100275. https://doi.org/10.1016/j.rinma.2022.100275

Pacheco-Torgal F., Castro-Gomes J., Jalali S.(2008). Alkali-activated binders : A review. Part 2. About materials and binders manufacture, *Construction and Building Materials*, 22(7), 1315-1322. https://doi.org/10.1016/j.conbuildmat.2007.03.019

Padavala S. S. A. B., Dey S., Veerendra G. T. N., Phani Manoj A. V. (2024) Experimental study on concrete by partial replacement of cement with fly ash and coarse aggregates with palm kernel shells (Pks) and with addition of hybrid fibers, *Chemistry of Inorganic Materials*, 2, 100033. https://doi.org/10.1016/j.cinorg.2024.100033

Payá J., Monzó J., Borrachero M. V., Díaz-Pinzón L., Ordóñez L. M. (2002) Sugar-cane bagasse ash (SCBA) : studies on its properties for reusing in concrete production, *Journal of Chemical Technology & Biotechnology*, 77(3), 321-325. https://doi.org/10.1002/jctb.549

Priya S. S., Padmanaban L.(2023) Effect of coconut shell ash as an additive on the properties of green concrete, *Global NEST Journal*, 26(1), 1-9. https://doi.org/10.30955/gnj.005413

Rajak M. A. A., Majid Z. A., Ismail M. (2015) Morphological characteristics of hardened cement pastes incorporating nano-palm oil fuel ash, *Procedia Manufacturing*, 2, 512-518. https://doi.org/10.1016/j.promfg.2015.07.088

Ranatunga K. S., Del Rey Castillo E., Toma C. L. (2023) Evaluation of the optimal concrete mix design with coconut shell ash as a partial cement replacement, *Construction and Building Materials*, 401, 132978. https://doi.org/10.1016/j.conbuildmat.2023.132978

Rukzon S., Chindaprasirt P. (2012) Utilization of bagasse ash in high-strength concrete, *Materials & Design*, 34, 45-50. https://doi.org/10.1016/j.matdes.2011.07.045

Salih M. A., Farzadnia N., Ali Ab. Abd., Demirboga R. (2015). Effect of different curing temperatures on alkali activated palm oil fuel ash paste, *Construction and Building Materials*, 94, 116-125. https://doi.org/10.1016/j.conbuildmat.2015.06.052

Sen S., Chandak R. (2015) Effect of coconut fibre ash on strength properties of concrete, *Int. Journal of Engineering Research and Applications*, 5(4), 33-35.

Silva E. J. D., Marques M. L., Velasco F. G., Fornari J. C., Luzardo F. M., Tashima M. M. (2017) A new treatment for coconut fibers to improve the properties of cement-based composites – Combined effect of natural latex/pozzolanic materials, *Sustainable Materials and Technologies*, 12, 44-51. https://doi.org/10.1016/j.susmat.2017.04.003

Sua-iam G., Chatveera B. (2021) A study on workability and mechanical properties of eco-sustainable self-compacting concrete incorporating PCB waste and fly ash, *Journal of Cleaner Production*, 329, 129523. https://doi.org/10.1016/j.jclepro.2021.129523

Tabaght, F. E., Azzaoui, K., Elidrissi, A., Hamed, O., Mejdoubi, E., Jodeh, S., … Lamhamdi, A. (2020). New nanostructure based on hydroxyapatite modified cellulose for bone substitute, synthesis, and characterization. *International Journal of Polymeric Materials and Polymeric Biomaterials*, 70(6), 437–448. https://doi.org/10.1080/00914037.2020.1725758

Tagnit-Hamou A., Tognovi T. M. (2012) Valorization of locally available industrial and agro-industrial wastes in concrete: a sustainable solution, *Journal of the Chinese Ceramic Society*, 43(10), 1372-1384. http://dx.doi.org/10.14062/j.issn.0454-5648.2015.10.07

Taku K. (2012) Coconut shell ash as partial replacement of ordinary portland cement in concrete production, *International Journal of Scientific & Technology Research*, 1(8), 86-89.

Teja K. V., Sai P. P., Meena T. (2017) Investigation on the behaviour of ternary blended concrete with scba and sf, *IOP Conference Series: Materials Science and Engineering*, 263(3), 032012. https://doi.org/10.1088/1757-899X/263/3/032012

Thomas B. S., Yang J., Mo K. H., Abdalla J. A., Hawileh R. A., Ariyachandra E. (2021) Biomass ashes from agricultural wastes as supplementary cementitious materials or aggregate replacement in cement/geopolymer concrete : A comprehensive review, *Journal of Building Engineering*, 40, 102332. https://doi.org/10.1016/j.jobe.2021.102332

Umamaheswari R., Vigneshkumar M. (2018) Experimental study on partial replacement of cement with coconut shell ash and silica fume in concrete, *International Research Journal of Engineering and Technology (IRJET)*, 05(07), 2175-2179.

Vasanthi P., Selvan Se. S., Murthi P., Reddy Ra. I., Poongodi K. (2020) Impact of Partial Replacement of Cement by Coconut Shell Ash and Coarse Aggregate by Coconut Shell on Mechanical Properties of Concrete, *IOP Conference Series: Materials Science and Engineering*, 981(3), 032080. https://doi.org/10.1088/1757-899X/981/3/032080

Zeyad A. M., Johari Me. A. M., Tayeh B. A., Yusuf M. O. (2016) Efficiency of treated and untreated palm oil fuel ash as a supplementary binder on engineering and fluid transport properties of high-strength concrete, *Construction and Building Materials*, 125, 1066-1079. https://doi.org/10.1016/j.conbuildmat.2016.08.065

Zeyad A. M., Johari Me. A. M., Tayeh B. A., Yusuf M. O. (2017) Pozzolanic reactivity of ultrafine palm oil fuel ash waste on strength and durability performances of high strength concrete, *Journal of Cleaner Production*, 144, 511-522. https://doi.org/10.1016/j.jclepro.2016.12.121

(2025) ; http://www.jmaterenvironsci.com